Volatility Measurements of Individual Components in Organic Aerosol Mixtures Using Temperature Programmed Desorption – Direct Analysis in Real Time – High Resolution Mass Spectrometry

Christopher P. West, ¹ Yun-Jung Hsu, ¹ Killian T. MacFeely, ¹ Shelby M. Huston, ¹ Bianca P. Aridjis-Olivos, ¹ Ana C. Morales, ¹ Alexander Laskin ^{1,2*}

ABSTRACT: Atmospheric organic aerosols (OA) have profound effects on air quality, visibility, and radiative forcing of climate. Quantitative assessment of gas-particle equilibrium of OA components is critical to understand formation, growth, distribution, and evolution of OA in the atmosphere. This study presents a novel ambient pressure measurement approach developed and tested for untargeted screening of individual components in complex OA mixtures, followed by targeted chemical speciation of identified species, and assessment of their physicochemical properties such as saturation vapor pressure and enthalpies of sublimation/evaporation. The method employs temperature programmed desorption (TPD) experiments coupled to 'direct analysis in real time' (DART) ionization source and high-resolution mass spectrometry (HRMS) detection. Progression of the mass spectra is acquired in the TPD experiments over T = 25-350 °C temperature range and extracted ion chromatograms (EIC) of individual species are used to infer their apparent enthalpies of sublimation/evaporation (ΔH^*_{sub}) and saturation vapor pressure $(p_T^*, partial partia$ organic compounds with known ΔH_{sub} and C_T , values, which showed excellent agreement between our results and the existing data. We then extend these experiments to interrogate individual components in complex OA samples generated in the laboratory-controlled ozonolysis of α -pinene, limonene and β -ocimene monoterpenes. The abundant OA species of interest are distinguished based on their accurate mass measurements, followed by quantitation of their apparent ΔH^*_{Sub} and C^*_T , values from the corresponding EIC records. Comparison of C*298K values derived from our experiments for the individual OA components with the corresponding estimates based on their elemental composition using a 'molecular corridors' (MC) parameterization suggests that the MC calculations tend to overestimate the saturation vapor pressures of OA components. Presented results indicate very promising applicability of the TPD-DART-HRMS method for the untargeted analysis of organic molecules in OA and other environmental mixtures, enabling rapid detection and quantification of organic pollutants in the real-world condensed-phase samples at atmospheric pressure and without sample preparation.

INTRODUCTION

Organic aerosols (OA) account for a large fraction of airborne particulate matter in the atmosphere, contributing to $\sim 20-90\%$ of the total mass of aerosol in the sub micrometer range. 1,2 Sources of OA include primary OA emissions from industry and transportation and secondary OA formed by the multiphase photochemical oxidation reactions of volatile organic compounds. 1,2 OA contain large number of individual compounds with broad variability in their elemental composition, molecular weights and structures. During atmospheric ageing composition of OA continues to evolve, driven by various reactions and processes, including gas-particle partitioning of organic species which drive formation and mass growth of OA. 3 Quantitative description of the gas-particle partitioning in OA for atmospheric models requires input data on the saturation vapor pressure of individual OA components.

The saturation vapor pressure of individual chemical species based on the IUPAC definition⁴ is: "a thermodynamic quantity where the pressure exerted by a pure substance at a given temperature in a system containing only the vapor and condensed phase (solid or liquid) of that substance in thermodynamic equilibrium." The saturation vapor pressure ${}^{i}p_{T}^{0}$ of species i depends on its molecular interactions in the condensed phase and on the temperature (T) of the system.⁵ Quantitative measurements of p_T^0 and enthalpy of sublimation/evaporation (ΔH_{sub}), two key intrinsic thermodynamic properties describing the equilibrium gas-particle partitioning of organic compounds, are necessary to inform atmospheric models.⁶ Experimental measurements of ${}^{i}p_{T}^{0}$ and ${}^{i}\Delta H_{sub}$ values describing the OA components is a very challenging task because of the inherent chemical complexity of the samples, the non-ideal behavior of these mixtures, and the diffusion kinetic transport limitations in the condensed phase.⁷

A large volume of experimental data on the ${}^{i}p_{T}^{0}$ and ${}^{i}\Delta H_{sub}$ values has been accumulated in the last two decades based on the targeted measurements of selected individual organic compounds i.6 These studies employed various methods of Knudsen cells, 8–10 single particle electrodynamic balance, 11-13 optical tweezers, 14 tandem differential mobility analyzers, 15-20 and vacuum-based temperature programmed desorption methods. 7,21-24 More recent development of a filter inlet for gases and aerosols²⁵ coupled to chemical ionization mass spectrometer utilized thermal desorption and detection of untargeted OA components from filter samples collected in laboratory and field studies. 26,27 That method allowed assessment of volatility classes and thermal stabilities of individual OA species inferred from the experimentally observed temperatures (T_{max}) corresponding to the maxima of the ions' intensity.²⁶ Consequently, estimations of saturation vapor pressure for the observed species were performed based on the comparison of experimental results with predictions by available semi-empirical models.^{28,29} While significant advances in the knowledge about gas-particle partitioning of OA have been provided by the existing measurement methods, further developments are much needed to establish new experimental techniques capable to probe systems approaching complexity of the real-world atmospheric mixtures.⁶

Here, we present an experimental method that allows direct measurements of apparent of p_T^* and ΔH^*_{sub} values for individual components present in the laboratory generated OA samples. (Herein, * and 0 symbols are used to distinguish apparent and intrinsic values). The presented method employs thermal evaporation of OA samples placed on the temperature programmed desorption (TPD) stage combined with the direct analysis in real time (DART) $^{30-32}$ ionization source and coupled to high resolution mass spectrometry (HRMS) for untargeted detection of OA components. We validate this method in experiments using a set of carboxylic acid standards and show that their experimentally

¹Department of Chemistry, Purdue University, West Lafayette, IN, 47907, USA

²Department of Earth, Atmospheric & Planetary Sciences, Purdue University, West Lafayette, IN, 47907, USA

measured p_T^* and ΔH^*_{sub} values match closely those of the corresponding p_T^0 and ΔH_{sub} reported in the literature. We then demonstrate utility of this method for untargeted analysis of individual species in multi-component OA samples generated by ozonolysis of selected terpenes. We report apparent ${}^ip_T^*$ and ${}^i\Delta H^*_{sub}$ values for major identified species i obtained from a single analytical run and compare with their predicted values from 'molecular corridors' (MC) model²⁸ estimates. Experimental simplicity, analysis at ambient pressure over short period of time (minutes), no requirements for special sample preparation are important tenets of the presented method, which make it a practical top-down tool to study gas-particle partitioning of complex mixtures.

EXPERIMENTAL METHODS

Secondary organic aerosols (PSOA, LSOA, OSOA) were generated in laboratory experiments of the ozone-initiated oxidation of α -pinene, limonene, and β -ocimene, respectively. OA samples were collected on polytetrafluoroethylene filters by vacuum pulled filtration.³⁴ Detailed descriptions of the laboratory experiments, sample collection and storage are included in Supplementary Note 1, Figure S1. Portions of the OA samples were loaded individually onto copper pot stubs used in the TPD experiments. The TPD experiments were set as following: 0.4 min hold at 25°C, linear ramp at 70 °C min⁻¹ to 350 °C (0.4-5.0 min), and 2.0 min hold at 350 °C. HRMS measurements were performed using the Q-Exactive HF-X Orbitrap mass spectrometer interfaced with the TPD-DART setup. Further details of the TPD-DART-HRMS experiments are included in Supplementary Note 2. Supplementary Note 3 summarizes details of the data analysis, and Supplementary Note 4 contains summary of validation experiments with carboxylic acid standards.

RESULTS & DISCUSSION

Figure 1 illustrates representative results obtained in the TPD-DART-HRMS experiment with PSOA sample and the associated data processing workflow. In each experiment, progression of the mass spectra is recorded as a TPD chromatogram (Fig. 1a), whereas accurate mass measurements using HRMS provide untargeted identification of individual components through assignments of their elemental formulas. Extracted ion chromatograms (EIC) of abundant individual species are then analyzed to determine T^*_{max} temperatures characteristic of their highest $(I_T - I_{T_0})$ intensity (Fig. 1b), which is a difference between EIC signal recorded during (I_T) and before (I_{T_0}) the TPD run, starting from T_0 = 298K. Then, the EIC records are plotted as Arrhenius plots of $\ln(I_T - I_{T_o})$ versus 1/T to yield component-specific ΔH^*_{sub} values based on fitting (eq. E1) of the linear portion of plots (above the background level of I_{T_0}) with the Clausius-Clapeyron equation (Fig. 1c), resembling methodology of the vacuum-based TPD experiments.21

$$\ln(p_T^*) \sim \ln(I_T - I_{T_0}) = -\frac{\Delta H_{Sub}^*}{p_T} + Const$$
 E1

DART ionization uses electronically excited helium atoms (He*) that induce Penning ionization (He* + M \rightarrow He + M^{+•} + e^-), followed by a sequence of additional ion-molecule and electron-molecule reactions of analyte and common ambient species (i.e. O_2 , H_2O , N_2 and NH_3), forming a range of positive and negative ions.³⁵ The most abundant ions of the OA analyte ($C_xH_yO_z$) were observed as deprotonated species, $[C_xH_{y-1}O_z]^-$. Importantly, DART ambient ionization also produces significant amount of H[•], O[•] and [•]OH[•] fast radicals. Increase of the analyte supply during the TPD ramp will promote propagation of radical formation and

establishment of the stable radical pool, which will trigger fast consumption of analyte by reactions resembling combustion chemistry, as illustrated in Supplemental Note 3.

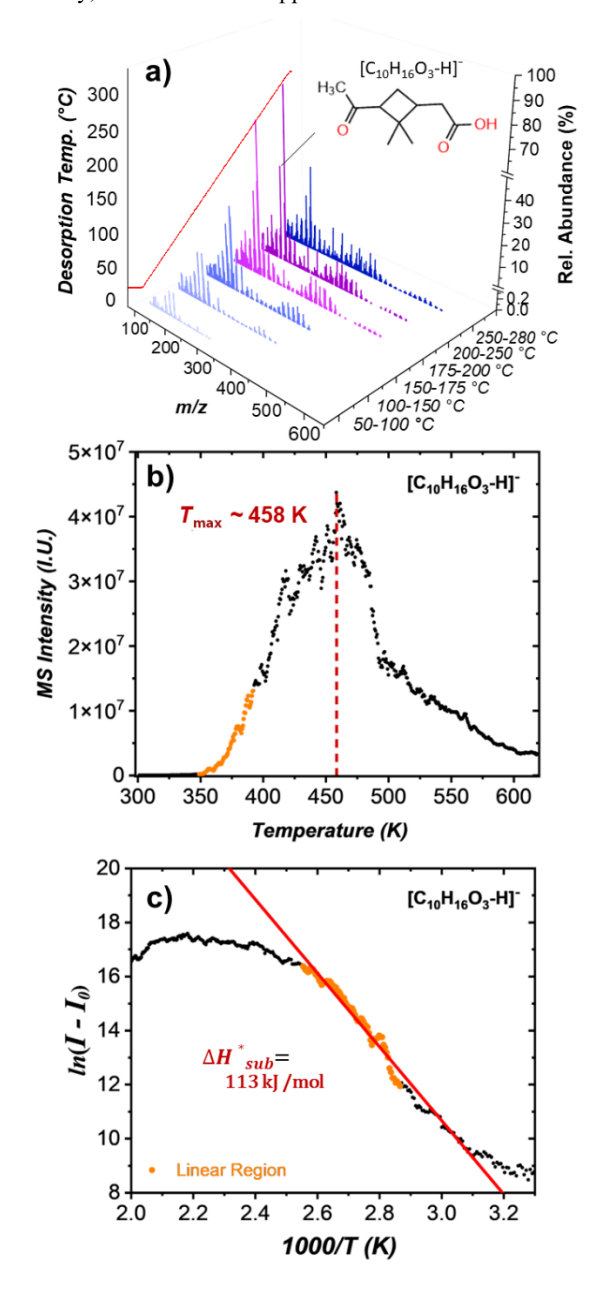


Figure 1. a) Progression of (–)DART-HRMS spectra of an PSOA sample averaged over annotated temperature ranges of the TPD experiment. The temperature profile (red) is shown along the second y-axis of the plot. b) An illustrative extracted ion chromatogram (EIC) of $[C_{10}H_{15}O_3]^-$ ion (deprotonated pinonic acid or its isomer). c) An Arrhenius plot of a logarithm of the EIC intensity $\ln(I-I_0)$ versus 1000/T (K) of $[C_{10}H_{15}O_3]^-$ ion. The linear region is used to fit the Clausius-Clapeyron equation and calculate the corresponding apparent ΔH^*_{sub} value shown in the plot.

Assuming reaction chemistry resembling combustion, we hypothesized that DART ion source may operate as a 'torch' igniting hydrocarbon/oxygen mixtures as they reach the flammability limit (also known as the flash point, T_{flash}). The latter is defined as

an experimentally observed minimum temperature at which the vapor concentration above the surface of liquid/solid hydrocarbon is high enough to form an ignitable mixture. If this hypothesis was correct, it would follow that values of T^*_{max} observed in our experiments (Fig. 1b) would therefore correlate with T_{flash} of analytes, i.e. $T^*_{max} \approx T_{flash}$. To validate this hypothesis, we conducted experiments with seven C₅-C₂₀ carboxylic acid standards and compared our experimental observations with the literature reported values of p_T^0 , ΔH_{sub} and T_{flash} . Complete list of the standards, their literature-reported properties, $^{6,10,14,17,20,22-24}$ and detailed account of the validation experiments are included in Supplemental Note 4. Comparison between T^*_{max} and T_{flash} observed for the standards (Fig. S3), showed overall consistency with less than ± 25 K difference between them.

Experimentally supported assumption of ${}^{i}T^{*}_{max} \approx {}^{i}T_{flash}$ allows to calculate the corresponding saturation vapor pressure of C_xH_y O_z assuming ${}^{i}p^{*}_{T_{max}} \approx {}^{i}p^{*}_{f_{flash}}$, where the latter is determined from the stoichiometry of reactions describing the complete combustion of $C_xH_yO_z$ species i at ambient conditions of 1 atm, using Equation S2 (Supplementary Note 3). For the calculations of ${}^{i}p^{*}_{T_{max}}$ presented in this work, we use ${}^{i}\phi = 1$ as an upper limit estimate, even though gas-phase mixtures of hydrocarbon species become flammable at lower vapor pressure and equivalence ratios of $\phi \sim 0.5.^{36}$ Therefore, for each specie i assigned with the neutral elemental formula of $C_xH_yO_z$, we observe ${}^{i}T^{*}_{max}$ (Fig. 1b), derive ${}^{i}\Delta H^{*}_{sub}$ from the linear fit of Arrhenius plot (Fig, 1c) and calculate ${}^{i}p^{*}_{T_{max}}$ using eq. E2. These values are then used to calculate saturation vapor pressure ${}^{i}p^{*}_{T}$ as a function of experimental temperature (T), using integrated form of the Clausius Clapeyron equation E2.

$$^{i}p_{T}^{*} = ^{i}p_{T_{max}}^{*} \times \exp\left[\left(-\frac{^{i}\Delta H_{sub}^{*}}{R}\right)\left(\frac{1}{T} - \frac{1}{T_{max}^{*}}\right)\right]$$
 E2

Obtained values of the saturation vapor pressure ${}^{i}p_{T}^{*}$ (Pa) are also reported as the corresponding gas-phase saturation mass loadings ${}^{i}C_{T}^{*}$, calculated based on the ideal gas equation (Supplementary Note 4, eq S3). Here, we use values of both ${}^{i}p_{T}^{*}$ and ${}^{i}C_{T}^{*}$ interchangeably, as needed to facilitate direct comparison with previous experimental data reported as p_{T}^{0} and MC modeling 28,37 results reported as C_{298K}^{0} .

Correlation plots of the apparent $\log^{i}C_{298K}^{*}$ and ${}^{i}\Delta H_{sub}^{*}$ values derived from our experiments for the set of carboxylic acids standards versus their literature^{6,10,14,17,20,22–24} values are included in Supplementary Note 4, Fig S4. They indicate that values obtained in our experiments agree very well with the literature data. Furthermore, extrapolation of p_{τ}^* values from the temperatures of this study into the lower temperatures employed in previous works shows remarkable agreement for five standards (decanoic (C₁₀), pentadecanoic (C₁₅), heptadecanoic (C₁₇), nonadecanoic (C₁₉) and eicosanoic (C₂₀) acids) illustrated in Figure S5. For these five species, cumulative combination of our results and the literature reported data exhibit close agreement that covers 5-7 orders of magnitude for the ${}^{i}p_{\tau}^{*}$ values over broad temperature intervals within 300-400 K range. For glutaric (C5) and cispinonic (C₁₀) acids, ΔH^*_{sub} values of our study corroborate very well the literature data (Fig. S4b). For glutaric acid, p_T^* values reported here agree well with a subset¹⁴ of the previous reports. Though, significant inconsistency exists between experimental studies of glutaric acid (Fig S5a). For *cis*-pinonic acid, p_{τ}^* values of our study are by a factor of 101-102 higher than the literature reports, which is the only case of significant discrepancy (Fig. S5b, Fig. S4a). However, two previous studies of *cis*-pinonic acid

also reported values of p_T^* differ by a factor of 10 (Fig. S5b), which make comparison ambiguous. Altogether, we conclude that methodology presented here can be plausibly applied to investigate apparent volatilities of untargeted components comprising complex organic mixtures.

Experiments with the OA samples were carried out to demonstrate performance of the TPD-DART-HRMS method to measure apparent values of ${}^{i}p_{\tau}^{*}$ and ${}^{i}\Delta H^{*}_{sub}$ for individual components in complex organic mixtures. Figure 2 shows correlation between experimentally derived values of $\log^i C^*_{298K}$ versus modeling predictions by an empirical MC method.²⁸ Presented data reports values for monomer, dimer and trimer components of OA, which contain between C₆ and C₂₉ carbon atoms (see Supplemental Note 5, Table S2). Their corresponding ${}^{i}C_{29RK}^{*}$ values span a broad range of 10^{-11} - 10^{4} µg m⁻³ and comprise all volatility bins commonly assumed in atmospheric models.3 Overall correlation trend between experimental and calculated datasets is readily observed, suggesting systematic overestimation of ${}^{i}C^{*}_{298K}$ values by the MC calculations. Observed discrepancy between the experimental data and the MC calculations is less significant for the IVOC species, where calculations overestimate experiments by a factor of ~10. However, for the ELVOC species, overestimations by the MC calculations appear to be more substantial, by factors as high as 10²-10³. Considering that values reported here are the upper limits, MC bias for higher volatilities might be even more significant.

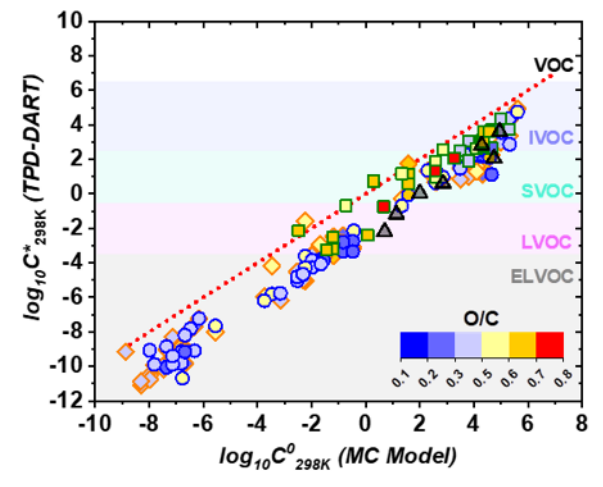


Figure 2. Correlation plot of log10€299K values derived from the TPD-DART-HRMS experiments versus predictions by the by the MC28 model for individual components identified in PSOA (orange diamonds), LSOA (blue circles) and OSOA (olive squares) samples. Inner areas of symbols are color-coded with respect to the O/C ratios of the corresponding species. Black triangles show values corresponding to seven carboxylic acid standards. Background colors indicate volatility ranges of volatile organic compounds (VOC), intermediate (IVOC), semi-volatile (SVOC), low-volatility (LVOC), and extremely low volatility (ELVOC). Dashed line indicates 1:1 correlation.

Assignments of individual OA components with elemental formulas based on the HRMS measurements allowed us to assess trends of the apparent C^*_{298K} and ΔH^*_{sub} values as a function of molecular size and O/C ratios specific for the individual OA components. Figure 3 summarizes these assessments for SOA components and the mono carboxylic acid standards. As expected, the saturation vapor pressure (shown as C^*_{298K}) systematically decreases for both larger species and species with higher O/C ratios.

With respect to the OA composition, monomer components are observed within IVOC and SVOC bins, dimers within LVOC and ELVOC bins, trimers are solely within ELVOC bin. For molecules with the same number of carbon atoms, variations in their O/C ratios between 0.2 and 0.7 result in up to a factor of $\sim 10^2$ differences between the corresponding C^*_{298K} values (Fig. 3a). Slopes of the linear fits of the experimental data shown in Figure 3a are consistent with relevant predictions by group contribution models.^{29,38} Specifically, the slope of -0.45 obtained from fitting the monocarboxylic acids data is in close agreement with SIM-POL.1²⁹ (-0.438) and EVAPORATION³⁸ (-0.501) predictions corresponding to addition of C atom to an aliphatic chain. However, the slope of -0.64 obtained for the SOA dataset is somewhat steeper, which reflects additional changes in O/C and DBE values in larger SOA components.²⁹ ΔH^*_{sub} values also show systematic scaling with molecular size and O/C ratios. Between monomer, dimer and trimer OA components, apparent sublimation enthalpies increase in steps of ~75 kJ/mol, connecting corresponding enthalpy ranges of 50-125, 125-200 and 200-275 kJ/mol, respectively. For the same size of compounds (same number of carbon atoms), increase in O/C ratio between 0.2 and 0.7 leads to enthalpy rise by also ~75 kJ/mol. Apparent volatility of dimers and trimers measured in the TPD experiment may be affected by thermal fragmentation of O-O linkages in the oligomeric structures.,²⁷ These would underestimate apparent volatility of oligomers and overestimate volatility of monomers. Knowledge of these component-specific properties is critical for modeling the gas-particle partitioning behavior of atmospheric OA, which can be plausibly advanced based on the TPD-DART-HRMS measurements presented here.

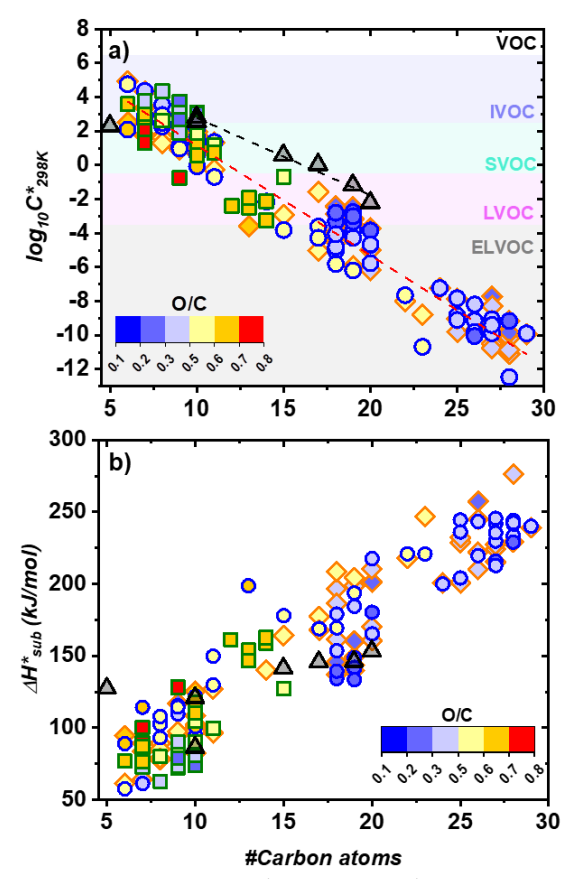


Figure 3. Values of a) $log_{10}C^*_{298K}$ and b) ΔH^*_{sub} obtained for individual OA components, plotted as a function of number of their carbon atoms and O/C ratios. Data include PSOA (orange dia-

monds), LSOA (blue circles), OSOA (olive squares) species, and aliphatic carboxylic acid standards (black triangles). Inner areas of symbols are color-coded with respect to the O/C ratios. In panel a, background colors indicate volatility ranges of volatile organic compounds (VOC), intermediate (IVOC), semi-volatile (SVOC), low-volatility (LVOC), and extremely low volatility (ELVOC).³ The slope of the linear fits (dashed lines) in upper panel are -0.45 for monocarboxylic acids and -0.64 for SOA components.

CONCLUSIONS

We presented the first application of a TPD-DART-HRMS measurement method for the experimental quantitative analysis of saturation vapor pressures (p_{τ}^*) and sublimation/evaporation enthalpies (ΔH^*_{sub}) of individual untargeted species identified within complex multi-component OA mixtures. The ability to monitor evaporation dynamics of the individual species and simultaneously provide their molecular characterization in a single experimental run is the key advantage of the method. Other important benefits of the method are very minimal requirement for the sample preparation and that the experiments are conducted at ambient pressure. We validated utility of the method based on the analysis of standards with known volatility characteristics and demonstrated its practical application for the analysis of atmospherically relevant mixtures of organic compounds. However, broader applications of this method need further investigation. Future studies will be directed towards systematic evaluation of the applicability and the limitations of this method for analysis of other complex mixtures of organic compounds related to different research areas such as studying the evaporation of semi-volatiles from various mixtures of interest: e.g., persistent organic pollutants, paints, coatings, sealants, toner inks, pesticides, household cooking and cleaning agents, personal care, hygiene products, etc.

ASSOCIATED CONTENT

Supporting Information

The Supporting Information is available free of charge at

https://pubs.acs.org/doi/10.1021/ acs.analchem.XXXXX.

Additional information as mentioned in the text; SOA generation and sampling experiments, Experimental setup & data analysis, Auxiliary information on combustion chemistry relevant for data analysis, Summary of the literature reported values for standards and measurements with the standards, Tabulated summary of the volatility values reported for individual OA components (Supplemental Notes S1-S5); additional Figures S1-S4 and Tables S1-S2 illustrating supplemental notes (PDF).

List of EIC records of individual species retrieved from TPD-DART-HRMS experiments (XLSX)

AUTHOR INFORMATION

Corresponding Author

Alexander Laskin – Department of Chemistry, Purdue University, West Lafayette, Indiana 47907, United States; orcid.org/0000-0002-7836-8417; Email: alaskin@purdue.edu

Authors

Christopher P. West – Department of Chemistry, Purdue University, West Lafayette, Indiana, 47907, United States; orcid.org/0000-0001-9337-2820

Yun-Jung Hsu - Department of Chemistry, Purdue University, West Lafayette, Indiana, 47907, United States; orcid.org/0000-0001-8883-5659

Killian MacFeely – Department of Chemistry, Purdue University, West Lafayette, Indiana, 47907, United States; orcid.org/0009-0001-7556-3305

Shelby Huston – Department of Chemistry, Purdue University, West Lafayette, Indiana, 47907, United States; orcid.org/0009-0000-2195-9219

Bianca Aridjis-Olivos – Department of Chemistry, Purdue University, West Lafayette, Indiana, 47907, United States; orcid.org/0000-0001-7060-676X

Ana C. Morales – Department of Chemistry, Purdue University, Indiana, West Lafayette, 47907, United States; orcid.org/0000-0001-6969-2883

Author Contributions

C.P.W. and A.L. designed the overall project framework. C.P.W. led experimental and data analysis tasks with the assistance from Y.H., K.M., S.H. B.A.O, and A.C.M. The manuscript was written by C.P.W. and A.L. with contributions from all co-authors.

ACKNOWLEDGMENTS

The work was supported by the startup funds allocated to A.L by the Department of Chemistry at Purdue University and partial support by the National Science Foundation grant AGS-2039985 and by NOAA Climate Program Office's AC4 program grant NA22OAR4310195. C.P.W. acknowledges the Bilsland dissertation fellowship (PU).

REFERENCES

- (1) Hallquist, M.; Wenger, J. C.; Baltensperger, U.; Rudich, Y.; Simpson, D.; Claeys, M.; Dommen, J.; Donahue, N. M.; George, C.; Goldstein, A. H.; Hamilton, J. F.; Herrmann, H.; Hoffmann, T.; Iinuma, Y.; Jang, M.; Jenkin, M. E.; Jimenez, J. L.; Kiendler-Scharr, A.; Maenhaut, W.; McFiggans, G.; Mentel, T. F.; Monod, A.; Prévôt, A. S. H.; Seinfeld, J. H.; Surratt, J. D.; Szmigielski, R.; Wildt, J. The Formation, Properties and Impact of Secondary Organic Aerosol: Current and Emerging Issues. *Atmospheric Chem. Phys.* **2009**, *9* (14), 5155–5236. https://doi.org/10.5194/acp-9-5155-2009.
- (2) Kanakidou, M.; Seinfeld, J. H.; Pandis, S. N.; Barnes, I.; Dentener, F. J.; Facchini, M. C.; Van Dingenen, R.; Ervens, B.; Nenes, A.; Nielsen, C. J.; Swietlicki, E.; Putaud, J. P.; Balkanski, Y.; Fuzzi, S.; Horth, J.; Moortgat, G. K.; Winterhalter, R.; Myhre, C. E. L.; Tsigaridis, K.; Vignati, E.; Stephanou, E. G.; Wilson, J. Organic Aerosol and Global Climate Modelling: A Review. Atmospheric Chem. Phys. 2005, 5 (4), 1053–1123. https://doi.org/10.5194/acp-5-1053-2005.
- (3) Donahue, N. M.; Robinson, A. L.; Trump, E. R.; Riipinen, I.; Kroll, J. H. Volatility and Aging of Atmospheric Organic Aerosol. In *Atmospheric and Aerosol Chemistry*; McNeill, V. F., Ariya, P. A., Eds.; Topics in Current Chemistry; Springer Berlin Heidelberg: Berlin, Heidelberg, 2012; Vol. 339, pp 97–143. https://doi.org/10.1007/128 2012 355.

- (4) Calvert, J. G. Glossary of Atmospheric Chemistry Terms (Recommendations 1990). *Pure Appl. Chem.* **1990**, *62* (11), 2167–2219. https://doi.org/10.1351/pac199062112167.
- (5) Prausnitz, J. M.; Lichtenthaler, R. N.; Azevedo, E. G. de. Molecular Thermodynamics of Fluid-Phase Equilibria; Pearson Education, 1998.
- (6) Bilde, M.; Barsanti, K.; Booth, M.; Cappa, C. D.; Donahue, N. M.; Emanuelsson, E. U.; McFiggans, G.; Krieger, U. K.; Marcolli, C.; Topping, D.; Ziemann, P.; Barley, M.; Clegg, S.; Dennis-Smither, B.; Hallquist, M.; Hallquist, Å. M.; Khlystov, A.; Kulmala, M.; Mogensen, D.; Percival, C. J.; Pope, F.; Reid, J. P.; Ribeiro da Silva, M. A. V.; Rosenoern, T.; Salo, K.; Soonsin, V. P.; YliJuuti, T.; Prisle, N. L.; Pagels, J.; Rarey, J.; Zardini, A. A.; Riipinen, I. Saturation Vapor Pressures and Transition Enthalpies of Low-Volatility Organic Molecules of Atmospheric Relevance: From Dicarboxylic Acids to Complex Mixtures. Chem. Rev. 2015, 115 (10), 4115–4156. https://doi.org/10.1021/cr5005502.
- (7) Bruns, E. A.; Greaves, J.; Finlayson-Pitts, B. J. Measurement of Vapor Pressures and Heats of Sublimation of Dicarboxylic Acids Using Atmospheric Solids Analysis Probe Mass Spectrometry. J. Phys. Chem. A 2012, 116 (24), 5900–5909. https://doi.org/10.1021/jp210021f.
- (8) Ribeiro da Silva, M. A. V.; Monte, M. J. S.; Ribeiro, J. R. Vapour Pressures and the Enthalpies and Entropies of Sublimation of Five Dicarboxylic Acids. *J. Chem. Thermodyn.* 1999, 31 (8), 1093–1107. https://doi.org/10.1006/jcht.1999.0522.
- (9) Ribeiro da Silva, M. A. V.; Monte, M. J. S.; Ribeiro, J. R. Thermodynamic Study on the Sublimation of Succinic Acid and of Methyl- and Dimethyl-Substituted Succinic and Glutaric Acids. *J. Chem. Thermodyn.* 2001, 33 (1), 23–31. https://doi.org/10.1006/jcht.2000.0715.
- (10) Booth, A. M.; Barley, M. H.; Topping, D. O.; McFiggans, G.; Garforth, A.; Percival, C. J. Solid State and Sub-Cooled Liquid Vapour Pressures of Substituted Dicarboxylic Acids Using Knudsen Effusion Mass Spectrometry (KEMS) and Differential Scanning Calorimetry. *Atmospheric Chem. Phys.* 2010, 10 (10), 4879–4892. https://doi.org/10.5194/acp-10-4879-2010.
- (11) Price, C. L.; Kaur Kohli, R.; Shokoor, B.; Davies, J. F. Connecting the Phase State and Volatility of Dicarboxylic Acids at Elevated Temperatures. J. Phys. Chem. A 2022. https://doi.org/10.1021/acs.jpca.2c04546.
- (12) Davis, E. J.; Ray, A. K. Determination of Diffusion Coefficients by Submicron Droplet Evaporation. *J. Chem. Phys.* 1977, 67 (2), 414–419. https://doi.org/10.1063/1.434903.
- (13) Davis, E. J.; Ray, A. K. Submicron Droplet Evaporation in the Continuum and Non-Continuum Regimes. *J. Aerosol Sci.* **1978**, *9* (5), 411–422. https://doi.org/10.1016/0021-8502(78)90003-4.
- (14) Pope, F. D.; Tong, H.-J.; Dennis-Smither, B. J.; Griffiths, P. T.; Clegg, S. L.; Reid, J. P.; Cox, R. A. Studies of Single Aerosol Particles Containing Malonic Acid, Glutaric Acid, and Their Mixtures with Sodium Chloride. II. Liquid-State Vapor Pressures of the Acids. J. Phys. Chem. A 2010, 114 (37), 10156–10165. https://doi.org/10.1021/jp1052979.
- (15) Rader, D. J.; McMurry, P. H. Application of the Tandem Differential Mobility Analyzer to Studies of Droplet Growth or Evaporation. J. Aerosol Sci. 1986, 17 (5), 771– 787. https://doi.org/10.1016/0021-8502(86)90031-5.

- (16) Koponen, I. K.; Riipinen, I.; Hienola, A.; Kulmala, M.; Bilde, M. Thermodynamic Properties of Malonic, Succinic, and Glutaric Acids: Evaporation Rates and Saturation Vapor Pressures. *Environ. Sci. Technol.* 2007, 41 (11), 3926– 3933. https://doi.org/10.1021/es0611240.
- (17) Bilde, M.; Pandis, S. N. Evaporation Rates and Vapor Pressures of Individual Aerosol Species Formed in the Atmospheric Oxidation of α- and β-Pinene. *Environ. Sci. Technol.* **2001**, 35 (16), 3344–3349. https://doi.org/10.1021/es001946b.
- (18) Bilde, M.; Svenningsson, B.; Mønster, J.; Rosenørn, T. Even-Odd Alternation of Evaporation Rates and Vapor Pressures of C3-C9 Dicarboxylic Acid Aerosols. *Environ.* Sci. Technol. 2003, 37 (7), 1371–1378. https://doi.org/10.1021/es0201810.
- (19) Tao, Y.; McMurry, P. H. Vapor Pressures and Surface Free Energies of C14-C18 Monocarboxylic Acids and C5 and C6 Dicarboxylic Acids. *Environ. Sci. Technol.* 1989, 23 (12), 1519–1523. https://doi.org/10.1021/es00070a011.
- (20) Salo, K.; Jonsson, Å. M.; Andersson, P. U.; Hallquist, M. Aerosol Volatility and Enthalpy of Sublimation of Carbox-ylic Acids. *J. Phys. Chem. A* 2010, 114 (13), 4586–4594. https://doi.org/10.1021/jp910105h.
- (21) Chattopadhyay, S.; Tobias, H. J.; Ziemann, P. J. A Method for Measuring Vapor Pressures of Low-Volatility Organic Aerosol Compounds Using a Thermal Desorption Particle Beam Mass Spectrometer. *Anal. Chem.* 2001, 73 (16), 3797–3803. https://doi.org/10.1021/ac010304j.
- (22) Chattopadhyay, S.; Ziemann, P. J. Vapor Pressures of Substituted and Unsubstituted Monocarboxylic and Dicarboxylic Acids Measured Using an Improved Thermal Desorption Particle Beam Mass Spectrometry Method. *Aerosol Sci. Technol.* 2005, 39 (11), 1085–1100. https://doi.org/10.1080/02786820500421547.
- (23) Cappa, C. D.; Lovejoy, E. R.; Ravishankara, A. R. Determination of Evaporation Rates and Vapor Pressures of Very Low Volatility Compounds: A Study of the C4–C10 and C12 Dicarboxylic Acids. J. Phys. Chem. A 2007, 111 (16), 3099–3109. https://doi.org/10.1021/jp068686q.
- (24) Cappa, C. D.; Lovejoy, E. R.; Ravishankara, A. R. Evaporation Rates and Vapor Pressures of the Even-Numbered C8–C18 Monocarboxylic Acids. *J. Phys. Chem. A* 2008, 112 (17), 3959–3964. https://doi.org/10.1021/jp710586m.
- (25) Lopez-Hilfiker, F. D.; Mohr, C.; Ehn, M.; Rubach, F.; Kleist, E.; Wildt, J.; Mentel, T. F.; Lutz, A.; Hallquist, M.; Worsnop, D.; Thornton, J. A. A Novel Method for Online Analysis of Gas and Particle Composition: Description and Evaluation of a Filter Inlet for Gases and AEROsols (FI-GAERO). Atmospheric Meas. Tech. 2014, 7 (4), 983–1001. https://doi.org/10.5194/amt-7-983-2014.
- (26) Buchholz, A.; Ylisirniö, A.; Huang, W.; Mohr, C.; Canagaratna, M.; Worsnop, D. R.; Schobesberger, S.; Virtanen, A. Deconvolution of FIGAERO-CIMS Thermal Desorption Profiles Using Positive Matrix Factorisation to Identify Chemical and Physical Processes during Particle Evaporation. *Atmospheric Chem. Phys.* 2020, 20 (13), 7693–7716. https://doi.org/10.5194/acp-20-7693-2020.
- (27) Huang, Y.; Kenseth, C. M.; Dalleska, N. F.; Seinfeld, J. H. Coupling Filter-Based Thermal Desorption Chemical Ionization Mass Spectrometry with Liquid Chromatography/Electrospray Ionization Mass Spectrometry for Molecular Analysis of Secondary Organic Aerosol. *Environ. Sci. Technol.* 2020, 54 (20), 13238–13248. https://doi.org/10.1021/acs.est.0c01779.

- (28) Li, Y.; Pöschl, U.; Shiraiwa, M. Molecular Corridors and Parameterizations of Volatility in the Chemical Evolution of Organic Aerosols. *Atmospheric Chem. Phys.* 2016, 16 (5), 3327–3344. https://doi.org/10.5194/acp-16-3327-2016.
- (29) Pankow, J. F.; Asher, W. E. SIMPOL.1: A Simple Group Contribution Method for Predicting Vapor Pressures and Enthalpies of Vaporization of Multifunctional Organic Compounds. *Atmospheric Chem. Phys.* 2008, 8 (10), 2773– 2796. https://doi.org/10.5194/acp-8-2773-2008.
- (30) Cody, R. B.; Fouquet, T. N. J.; Takei, C. Thermal Desorption and Pyrolysis Direct Analysis in Real Time Mass Spectrometry for Qualitative Characterization of Polymers and Polymer Additives. *Rapid Commun. Mass Spectrom.* 2020, 34 (S2), e8687. https://doi.org/10.1002/rcm.8687.
- (31) Cody, R. B.; Laramée, J. A.; Durst, H. D. Versatile New Ion Source for the Analysis of Materials in Open Air under Ambient Conditions. *Anal. Chem.* 2005, 77 (8), 2297– 2302. https://doi.org/10.1021/ac050162j.
- (32) West, C. P.; Brown, H. M.; Fedick, P. W. Molecular Characterization of the Thermal Degradation of Per- and Polyfluoroalkyl Substances in Aqueous Film-Forming Foams via Temperature-Programmed Thermal Desorption—Pyrolysis—Direct Analysis in Real Time—Mass Spectrometry. Environ. Sci. Technol. Lett. 2023, 10 (4), 308–315. https://doi.org/10.1021/acs.estlett.3c00064.
- (33) Nizkorodov, S. A.; Laskin, J.; Laskin, A. Molecular Chemistry of Organic Aerosols through the Application of High Resolution Mass Spectrometry. *Phys. Chem. Chem. Phys.* 2011, 13 (9), 3612–3629. https://doi.org/10.1039/C0CP02032J.
- (34) West, C. P.; Mesa Sanchez, D.; Morales, A. C.; Hsu, Y.-J.; Ryan, J.; Darmody, A.; Slipchenko, L. V.; Laskin, J.; Laskin, A. Molecular and Structural Characterization of Isomeric Compounds in Atmospheric Organic Aerosol Using Ion Mobility-Mass Spectrometry. J. Phys. Chem. A 2023, 127 (7), 1656–1674. https://doi.org/10.1021/acs.jpca.2c06459.
- (35) Gross, J. H. Direct Analysis in Real Time—a Critical Review on DART-MS. *Anal. Bioanal. Chem.* 2014, 406 (1), 63–80. https://doi.org/10.1007/s00216-013-7316-0.
- (36) Liao, S. Y.; Cheng, Q.; Jiang, D. M.; Gao, J. Experimental Study of Flammability Limits of Natural Gas—Air Mixture. J. Hazard. Mater. 2005, 119 (1), 81–84. https://doi.org/10.1016/j.jhazmat.2004.09.031.
- (37) Li, Y.; Shiraiwa, M. Molecular Corridors, Volatility and Particle Phase State in Secondary Organic Aerosols. In Multiphase Environmental Chemistry in the Atmosphere; ACS Symposium Series; American Chemical Society, 2018; Vol. 1299, pp 209–244. https://doi.org/10.1021/bk-2018-1299.ch011.
- (38) Compernolle, S.; Ceulemans, K.; Müller, J.-F. EVAPO-RATION: A New Vapour Pressure Estimation Methodfor Organic Molecules Including Non-Additivity and Intramolecular Interactions. *Atmospheric Chem. Phys.* 2011, 11 (18), 9431–9450. https://doi.org/10.5194/acp-11-9431-2011.